ARTICLE

Simple and universal synthesis of sulfonated porous organic polymers with high proton conductivity

Received 00th January 20xx,
Accepted 00th January 20xx

DOI: 10.1039/x0xx00000x

Zhongping Li,*[a]† Yuze Yao,[a]† Dongjin Wang,[a]† Md. Mahmudul Hasan,[a] Athchaya Suwansoontorn,[a] He Li,*[b] Gang Du,[a] Zhaohan Liu,[a] and Yuki Nagao*[a]

Along with the rapid development of economic integration and regional economization worldwide, the growth of green and sustainable resources has posed a major concern. Proton-exchange membrane fuel cells (PEMFCs) are exemplary of green, resource-conserving, and environmentally protective energy resources. Porous organic polymers (POPs), a new class of porous material with high porosity, permanent pores, excellent stability, and easily modified functional units, can offer a good platform as proton-conducting electrolytes for fuel cells. However, a simple and general design to construct POPs with high proton conductivity presents a challenging project. For this study, we used simple benzene and aromatic benzene as building units through a facile and cost-effective process to create a series of POPs. We further prepared sulfonated POPs (S-POPs) with high-density sulfonic acid groups via post-sulphonation. S-POPs displayed excellent proton conductivity up to 10^{-2} S cm^{-1} at 25 °C and 95% relative humidity (RH), and high conductivity up to 10^{-1} S cm^{-1} at 80 °C and 95% RH, which ranked top among the most proton-conducting POPs. These results suggest that construction of S-POPs offers a simple and universal way to evolve structural designs for high proton-conductive materials.

Introduction

During the last few decades, human society has created a highly modern civilization reliant upon intensive use of fossil fuels, which have led to global environmental difficulties and threats to sustainable energy consumption. In light of those and other detrimental effects, developing effective technologies and new materials to provide green and sustainable resources is both urgent and necessary. Proton-exchange membrane fuel cells present some promise for clean energy systems that are compatible with environmental conservation.

Developed from Nafion as a current standard for PEMFCs, many researchers have designed sulfonated materials to improve proton conductivity.[1] Porous materials have an easily adjustable suitable structure and pore environment for proton conductivity.[2] For example, metal organic frameworks (MOFs) show high porosity, with designable pores and a skeleton.[3] However, only a few MOFs can be loaded with sulfonic acid groups including direct-design and post-synthesis because of their poor stability. Comparison of traditional porous materials demonstrates that POPs including conjugated microporous polymers (CMPs),[4a] polymers of intrinsic microporous (PIMs),[4b] covalent organic frameworks (COFs),[4c] porous aromatic frameworks (PAFs),[4d] and hypercrosslinked polymers (HCPs)[4e] generally exhibit good porosity, permanent pores, excellent stability, and various modified sites on walls, offering promise for multi-functional application such as gas uptake,[5–6] catalyst,[7–8] chemical sensors,[9–10] and proton conductivity.[11–15]

Proton conducting POPs can be designed according to several principles. Loading proton sources such as imidazole, triazole, phosphoric acid, and p-toluene sulfonic acid into pores of functional POPs has been a standard approach for proton conduction.[12–13] In 2015, Xiang and co-authors reported mesoporous polyimides networks that were constructed to load imidazole as proton carriers to produce a good proton-conducting material.[11a] The proton conductivity of polymers reaches 3.49×10^{-4} S cm^{-1} at 90 °C and a highly anhydrous condition. To develop highly conductive materials, imine-based COF with high porosity and excellent stability was exploited elaborately by Jiang's group to improve the loading amounts of imidazole and triazole, which displayed high proton conductivity (4.37×10^{-3} S cm^{-1}).[11b] Banerjee and co-workers systematically studied a series of porous polymers with phosphoric acid for proton conduction.[12] Recently, they made a crystalline porous polymer into self-standing and flexible membrane with p-toluene sulfonic acid, which suggested excellent proton conductivity up to 7.8×10^{-2} S cm^{-1}.[12b] The proton-conductive porous polymers were also established by direct synthesis through building units with sulfonic acid units.[13] For example, Zhao and co-authors presented polymers decorated with pendant sulfonic acid groups. At 298 K and 97% relative humidity (RH), these frameworks exhibited intrinsic proton conductivity as high as 3.96×10^{-2} S cm^{-1}. Recently, a

[a] School of Materials Science, Japan Advanced Institute of Science and Technology, 1-1 Asahidai, Nomi, Ishikawa 923-1292, Japan.
[b] State Key Laboratory of Catalysis, Dalian Institute of Chemical Physics, Chinese Academy of Sciences, China.
† Z. Li, Y. Yao and D. Wang contributed equally.
*Corresponding author. E-mail address: lizp@jaist.ac.jp; lihe@dicp.ac.cn; ynagao@jaist.ac.jp.
Electronic Supplementary Information (ESI) available: [details of any supplementary information available should be included here]. See DOI: 10.1039/x0xx00000x

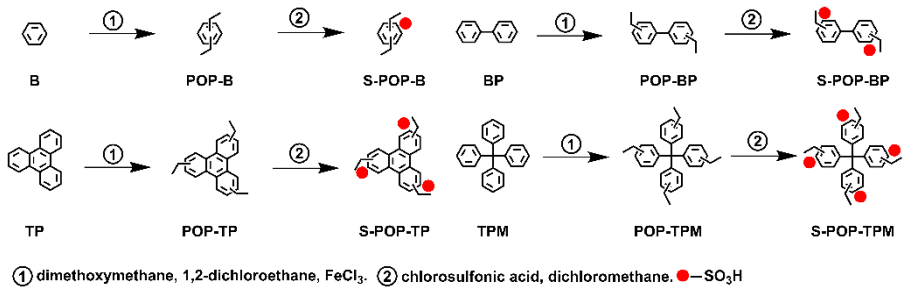

Scheme 1. Schematic representation of POP and S-POP synthesis.

post-sulphonation method to introduce sulfonic acid groups into frameworks has received much attention because of cost-effective processing. Hong's, Senker's, Ghosh's and Han's group achieved post-synthesis of a sulfonated porous organic polymers via chlorosulfonic acid.[14-15] Although design and synthesis of functional proton-conductive POPs have made great progress during the past years, crucially important issues such as simplicity and universality remain unresolved from the viewpoint of practical application.[12–15]

A strong demand exists to break through that limitation. Porous organic hyper-crosslinked polymers have been constructed using a facile and low-cost method via Friedel–Crafts alkylation of aromatic monomers using formaldehyde dimethyl acetal (FDA) as a crosslinker and $FeCl_3$ as catalyst.[4e] We are interested in this finding because they afford permanent pore structure and high porosity for porous polymers; the polymers can also be prepared easily to produce functional units through simple synthesis. In this research, we used simple and various aromatic benzene including two-dimensional (2D) molecules (benzene, B; biphenyl, BP; triphenylene, TP) and three-dimensional (3D) monomer (tetraphenylmethane, TPM) as building units through a facile process to afford diverse POPs, which were further decorated with high-density sulfonic acid groups via post-sulphonation (Scheme 1). The S-POPs displayed state-of-the-art high conductivity up to 10^{-2} S cm^{-1} at 25°C and 95% RH and 10^{-1} S cm^{-1} at 80 °C and 95% RH, which ranked remarkable performance among the most proton-conducting POPs.

Results and discussion

POPs can be prepared in high yield (98-99%) from simple benzene and aromatic monomer through Friedel–Crafts alkylation by using formaldehyde dimethyl acetal (FDA) as a crosslinker under the catalysis of $FeCl_3$, which is a reliable method to synthesis of highly porous POPs.[16] The S-POPs were conducted through post-synthesis by chlorosulfonic acid.[15] The success of polymers was confirmed by Fourier transforms infrared (FT IR) measurements. The FT IR spectra displayed readily apparent signals around 2913 and 3106 cm^{-1} for POP-B, 2920 and 3021 cm^{-1} for POP-PB, 2919 and 3026 cm^{-1} for POP-TP, and 2922 and 3024 cm^{-1} for POP-TPM, respectively, corresponding to C–H stretching vibration, thereby indicating occurrence of the connection (–CH_2–) of building units and formaldehyde dimethyl acetal (Fig. S1). Strong new peaks at 1173 and 1370 cm^{-1} for S-POP-B, 1172 and 1372 cm^{-1} for S-POP-BP, 1173 and 1371 cm^{-1} for S-POP-TP, 1174 and 1369 cm^{-1} for S-POP-TPM, respectively, can originate from the structure of S=O=S symmetric and asymmetric stretching modes. These results indicate the successful introduction of sulfonic acid groups by post-synthesis method. X-ray photoelectron spectroscopy (XPS) results of S-POP displayed C1s, O 1s, S 2s and 2p signals (Figs. 1a–1d). In Figs. 1e–1h, bonding energies of S $2p_{3/2}$ and S $2p_{1/2}$ of S-POPs were found around 168.2 and 169.3 eV, respectively, which further suggests the presence of sulfonic acid groups in the frameworks. The POPs and S-POPs showed no information of the Fe characteristics (Figs. 1i–1l), which meant that the catalyst can be removed by purification processing. Elemental mapping by energy dispersive spectroscopy (EDS) analysis of polymers was investigated for POPs and S-POPs (Fig. S2a–d). EDS images of S-POPs indicated a uniform distribution of elemental sulphur. The amount of sulfonic acid group of S-POPs was estimated through acid–base titration. The S-POP-B and S-POP-BP showed high sulfonic acid amounts of 29 and 28 wt%. The slightly lower quantity was at 18 wt% for S-POP-TP, which is ascribed to sulfonated benzene inactivated reactivity of the conjugated structure. Comparison of the 2D building units reveals that the S-POP-TMP has higher sulfonic acid density at 36 wt% because the 3D structure displayed rigidity, extensive space, and weak conjugation /hyperconjugation to improve the sulphonation reaction activity. The sulfonation process for polymers decorated high-density sulfonic acid groups.

The thermal stability of polymers was investigated by thermogravimetric analysis (TGA) under a nitrogen atmosphere (Fig. S3). The POPs showed excellent thermal stability and kept up to 300 °C. The S-POPs were stable up to 200 °C. Before 100 °C, S-POPs lose water molecules. Field emission–scanning electron

ARTICLE

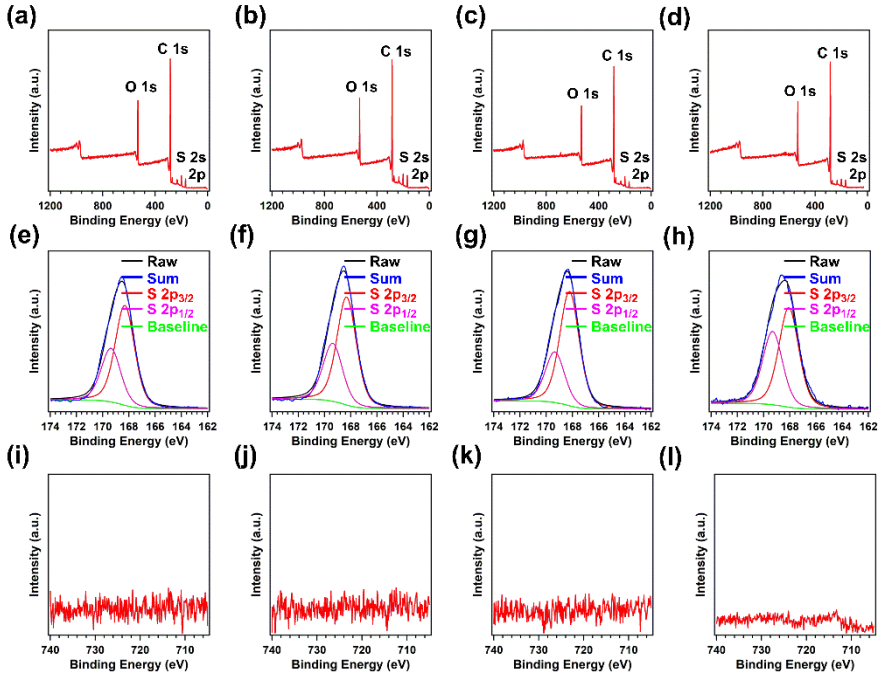

Fig. 1. X-ray photoelectron spectroscopy (XPS) spectra of (a) S-POP-B, (b) S-POP-BP, (c) S-POP-TP, and (d) S-POP-TPM. XPS analysis of S of (e) S-POP-B, (f) S-POP-BP, (g) S-POP-TP, and (h) S-POP-TPM. XPS analysis of Fe of (i) S-POP-B, (j) S-POP-BP, (k) S-POP-TP, and (l) S-POP-TPM.

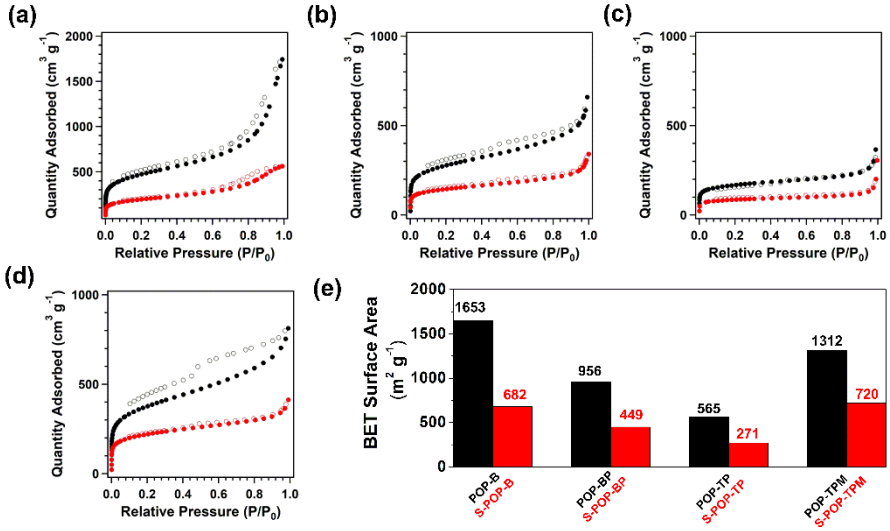

Fig. 2. Nitrogen sorption isotherms of (a) POP-B and S-POP-B, (b) POP-BP and S-POP-BP, (c) POP-TP and S-POP-TP, and (d) POP-TPM and S-POP-TPM measured at 77 K (●, adsorption; ○, desorption; black curves for POP and red curves for S-POP). (e) Comparison of BET surface area of POPs and S-POPs.

microscopy (FE–SEM) images were taken to elucidate the morphology of all the POPs (Fig. S4). It is particularly interesting that POP-BP and S-POP-BP revealed uniform micrometer-scale long rods (Figs. S4b and 4f). Powder X-ray diffraction measurements (PXRD) of all the POPs displayed no strong signals, which suggested their amorphous structure (Fig. S5).

The permanent porosities of POPs and S-POPs were investigated by nitrogen adsorption measurements taken at 77

K. POPs and S-POPs showed type I and type II isotherms with sharp uptake observed at low pressure (Figs. 2a–2d), which is a representative character of microporosity according to the IUPAC classification. The POP-B showed the highest Brunauer–Emmett–Teller (BET) surface area of 1653 $m^2 g^{-1}$. POP-BP, POP-TP, and POP-TPM also displayed high BET surface areas of 956, 565, and 1312 $m^2 g^{-1}$, respectively. After the post-sulphonation for polymers, the POP porosity also decreased, as shown in Fig. 2e. For example, S-POP-B showed a lower BET surface area, 683 $m^2 g^{-1}$, than that of POP-B (1653 $m^2 g^{-1}$). The BET surface areas of S-POP-BP, S-POP-TP, and S-POP-TPM were 449, 271, and 720 $m^2 g^{-1}$, respectively. The total volume calculated with nitrogen gas adsorbed at $P/P_0 = 0.99$ of POP-B, POP-BP, POP-TP, and POP-TPM was actuated respectively to be 2.68, 1.00, 0.63, and 1.26 $cm^3 g^{-1}$ (Fig. S6 a-d). The pore volumes of S-POPs were also reduced. S-POP-B, S-POP-BP, S-POP-TP, and S-POP-TPM exhibited pore volumes of 0.87, 0.53, 0.33, and 0.54 $cm^3 g^{-1}$, respectively. The lower porosity including BET surface area and pore volume was found in S-POPs, which indicated the sulfonic acids were successfully located on sulfonated polymers.

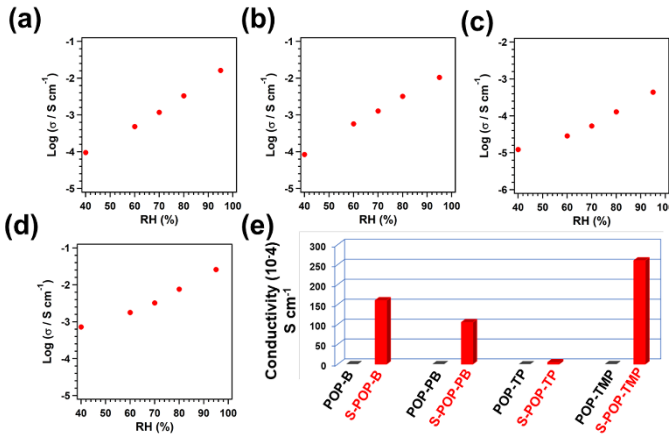

Fig. 3. Proton conductivities of (a) S-POP-B, (b) S-POP-BP, (c) S-POP-TP, and (d) S-POP-TPM measured at 25 °C under different RH. (e) Proton conductivities of POPs and S-POPs under 95% RH and 25 °C.

Humidity, a key point for a proton transport system, can promote and strengthen proton-exchange/transport efficiency. The water vapour sorption isotherms of POPs and S-POPs were measured at 298 K (Fig. S7a). Water adsorption capacities of 11.2, 10.4, and 17.9 mmol g^{-1} at $P/P_0 = 0.95$ were observed for POP-B, POP-BP, and POP-TPM, respectively. The lower water capture capability was observed at 7.5 mmol g^{-1} because of the hydrophobic conjugated units of POP-TP. Although S-POPs showed smaller BET specific surface areas and pore volumes than those of POPs, high water uptake of the S-POP-B, S-POP-BP, and S-POP-TP were found to be 36.1, 31.5 and 18.9 mmol g^{-1}, respectively (Figs. S7a and S7b). It is particularly interesting that S-POP-TPM exhibited higher water capture capability of 44.9 mmol g^{-1} because of the greater amount of sulfonic acid units in the skeleton, which possessed strong hydrophilic interaction towards the water molecule. The capture capability of all S-POPs was inferred as twice or three times that of the original POPs (Fig. S7b). For the number of water molecules adsorbed by per sulfonic acid group, each sulfonic acid molecule of S-POP-TPM can adsorb around 10.2 water molecules at $P/P_0 = 0.95$, which is lower than Nafion membranes such as Nafion 117 (21, 27 °C and liquid wafer), [17] and Nafion 211 (12, 25 °C and 95% RH).[18a]

The S-POPs displayed good porosity, remarkable water uptake, and high-density sulfonic acid units in the skeleton, which led us to measure the water-mediated proton conductivity. We firstly investigated the humidity dependence on proton conductivity for polymers from 40 to 95% RH at 25 °C. With the increment of humidity, the proton-conducting values of S-POPs were improved (Figs. 3a–3d and Figs. S8a–8d). For example, S-POP-B exhibited conductivities of 9.5×10^{-5}, 4.8×10^{-4}, 1.1×10^{-3}, and 3.3×10^{-3} S cm^{-1}, respectively, under 40%, 60%, 70%, and 80% RH at 25 °C (Fig. 3a). At 25 °C and 95% RH, high conductivity of S-POP-B was found at 1.5×10^{-2} S cm^{-1}, which is 3.4 orders of magnitude greater than that of POP-B under these conditions (Fig. 3e). The similar results were found for other polymers at 25 °C and 95% RH. For example, S-POP-BP also exhibited high proton conductivity of 1.0×10^{-2} S cm^{-1}, which is also a great increase in the original polymer (Figs. 3a and 3e). The lower conductivity of S-POP-TP was found at 4.4×10^{-4} S cm^{-1} as a result of poor water uptake and moderate density of proton sources in the skeleton (Fig. 3c). With high density of the proton source and excellent water uptake, remarkable conductivities of S-POP-TPM were recorded respectively on 7.2×10^{-4} (40% RH), 1.8×10^{-3} S cm^{-1} (60% RH), 3.3×10^{-3} S cm^{-1} (70% RH), and 7.6×10^{-3} S cm^{-1} (80% RH) at 25 °C. When the relative humidity was increased to 95% RH and 25 °C, the proton conductivity of S-POP-TPM was as high as 2.7×10^{-2} S cm^{-1}, which is ranked as having remarkable conductivity among the reported proton-conducting POPs.[14–15] The proton conductivities of POPs and S-POPs were measured at various temperatures under 95% RH and improved with increased temperature (Fig. S9). The conductivities of POP-B increased slightly to 4.5×10^{-4} (25 °C), 7.5×10^{-4} (60 °C), and 1.3×10^{-3} S cm^{-1} (80 °C) under 95% RH (Fig. S9a). With increasing temperature, S-POP-B also enhanced proton conductivity of 1.6×10^{-2} S cm^{-1} (25 °C), 3.9×10^{-2} (60 °C), and 6.4×10^{-2} (80 °C) (Fig. S9b). Also, S-POP-BP and S-POP-TP exhibited good proton-conducting performances of 4.1×10^{-2} and 4.6×10^{-3} at 80 °C and 95% RH, respectively (Figs. S9d and 9f). The S-POP-TPM showed excellent values as high as 1.0×10^{-1} S cm^{-1} at 80 °C and 95% RH (Fig. S9h). Compare to current standard materials such as Nafion 211 (1.3×10^{-1} S cm^{-1}, 80 °C, 95% RH) [18a] and Nafion 112 (1.4×10^{-1} S cm^{-1}, 65 °C, water), [18b] this result shows similarly high conductivity performance. We also have checked time-dependent proton conduction for S-POP-TPM and there is negligible change in proton conductivity even after 6 h (Fig. S10).

The activation energy (E_A) of proton conduction of POPs and S-POPs was ascertained from linear least-squares fitting of the slopes of Arrhenius plots at different temperatures. The E_A were found to be 0.61 eV for POP-B and 0.24 eV for S-POP-B (Fig. 4a). Comparison of the parent polymers, S-POP-BP, S-POP-TP, and S-POP-TPM also revealed the respectively lower E_A values of 0.26, 0.42, and 0.23 eV (Figs. 4b–4d). These results indicate that the mechanism for proton conduction is transported by the hopping pathway through extended hydrogen-bonding interaction between water molecules and sulfonic acid, which greatly enhanced the proton-transfer ability of polymers.

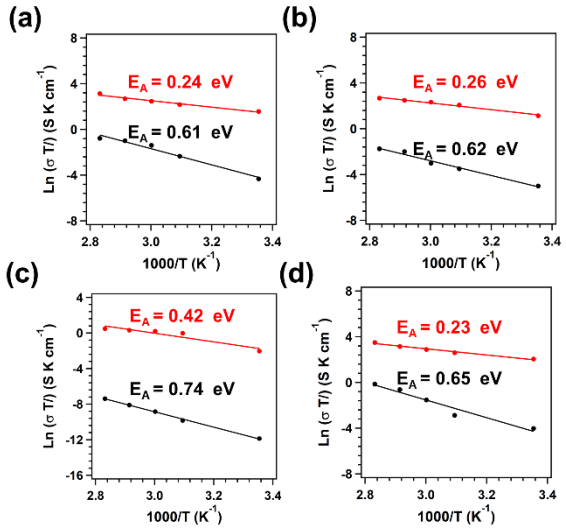

Fig. 4. Arrhenius plots for (a) POP-B and S-POP-B, (b) POP-BP and S-POP-BP, (c) POP-TP and S-POP-TP, (d) POP-TPM and S-POP-TPM (black curves for POP; red curves for S-POP).

Conclusions

In summary, we synthesized various porous organic polymers with high porosity through simple and cost-effective methods, which are suitable for most aromatic benzenes. Sulfonated porous organic polymers with high-density sulfonic acid groups were prepared through post-sulphonation, which enhanced the water uptake to be much greater than that of original POPs. It is particularly interesting that S-POP-TPM decorated high-density sulfonic acid amounts and exhibited remarkable water absorbability to offer high conductivity up to 10^{-2} S cm^{-1} at 25 °C and 95% RH, and 10^{-1} S cm^{-1} at 80 °C and 95% RH. Results of this study suggest that the construction of sulfonated POPs offers a simple and universal means of evolving a structural design for high proton-conductive materials.

Experimental

Synthesis of POPs: The POPs were synthesized using reported methods.[16] Benzene (B) (80 uL, 0.9 mmol), formaldehyde dimethyl acetal (159 uL, 1.8 mmol), anhydrous $FeCl_3$ (290 mg, 1.8 mmol) and 1,2-dichloroethane 4 mL were added the flask. The mixture was stirred for 1 min, and degassed through three freeze-pump-thaw cycles. The mixture was heated at 80 °C for 48 h under Argon atmosphere. The precipitate was collected and washed with water and acetone, and soxhleted by methanol overnight. The polymer was filtered and washed by water and acetone, stirred in HCl (1 M 25 mL) overnight, filtered and washed by water and acetone, and dried under vacuum at room temperature for 24 h to afford powder in 99% isolated yield. The synthesized process of POP-BP, POP-TP, and POP-TPM was similar to POP-B. After purification, POP-BP, POP-TP, and POP-TPM polymers were prepared with high yield of 98%, 99%, and 99%, respectively.

Synthesis of S-POPs: The S-POPs were synthesized using reported methods.[15] POP-B (200 mg) was suspended in dichloromethane 10 mL. The mixture was stirred at ice-water bath for 10 mins, and chlorosulfonic acid 2.5 mL was added dropwise into this system at an ice-water bath. Then, the mixture raised to room temperature and stirred for 7 d. This mixture was poured into 300 mL of ice water, and returned to room temperature. The S-POP-B was collected and washed by water and acetone, and dried under vacuum for 24 h (264 mg). The synthesis of S-POP-BP, S-POP-TP, and S-POP-TPM was the same as that of S-POP-B.

Proton conductivity measurements

S-POPs were carefully ground to enable its uniform. The thin pellets of S-POPs were prepared under the high pressure. The pellet was equipped with two Pt electrodes with two platinum wires connecting the outside. We investigated proton conductivity of the thin pellet through impedance spectroscopy measurements using a frequency response analyzer (SI1260; Solartron Analytical) equipped with a high-frequency dielectric interface (SI1260; Solartron Analytical). We controlled relative humidity and temperature condition by using a computer-controlled environmental test chamber (SH-221; Espec Corp.). Impedance data was recorded for frequencies between 1 Hz and 10 MHz, with an applied alternating potential of 50 mV. Proton conductivity (σ) was calculated as, $\sigma = L / (R \times S)$, where R denotes the resistance value obtained from the impedance, S and L respectively stand for the contact electrode area and the thickness of the membrane. The activation energy (EA) of S-POPs was calculated as, $\sigma T = \sigma_0 \times \exp(-E_A / (k_B \times T))$, where σ is the proton conductivity, σ_0 is the pre-exponential factor, k_B is the Boltzmann constant, and T is the temperature.

Conflicts of interest

There are no conflicts to declare.

Acknowledgements

Z.L. and Y.N. appreciate support from JSPS KAKENHI grant number JP18J13699 and JP18K05257.

Notes and references

1 (a) M. A. Hickner, H. Ghassemi, Y. S. Kim, B. R. Einsla and J. E. McGrath, Alternative polymer systems for proton exchange membranes (PEMs), *Chem. Rev*., 2004, **104**, 4587; (b) T. Higashihara, K. Matsumoto and M. Ueda, Sulfonated aromatic hydrocarbon polymers as proton exchange membranes for fuel cells, *Polymer*, 2009, **50**, 5341; (c) Y. Nagao, Proton-conductivity enhancement in polymer thin films, *Langmuir*, 2017, **33**, 12547; (d) Y. Nagao, Progress on highly proton-conductive polymer thin films with organized structure and molecularly oriented structure, *Sci. Tech. Adv. Mater*, 2020, **21**, 79.

2 (a) S. Horike, D. Umeyama and S. Kitagawa, Ion conductivity and transport by porous coordination polymers and metal–organic frameworks, *Acc. Chem. Res*., 2013, **11**, 2376; (b) M. Yoon, K. Suh, S. Natarajan and K. Kim, Proton conduction in

metal-organic frameworks and related modularly built porous solids, *Angew. Chem. Int. Ed*., 2013, **52**, 2688.
3 T. Yamada, K. Otsubo, R. Makiura and H. Kitagawa, Designer coordination polymers: dimensional crossover architectures and proton conduction, *Chem. Soc. Rev*., 2013, **42**, 6655.
4 (a) Y. Xu, S. Jin, H. Xu, A. Nagai and D. Jiang, Conjugated microporous polymers: design, synthesis and application, *Chem. Soc. Rev*., 2013, **42**, 8012; (b) Y. Zhang, and S. N. Riduan, Functional porous organic polymers for heterogeneous catalysis, *Chem. Soc. Rev*., 2012, **41**, 2083; (c) K. Geng, T. He, R. Liu, S. Dalapati, K. T. Tan, Z. Li, S. Tao, Y. Gong, Q. Jiang and D. Jiang, Covalent organic frameworks: design, synthesis, and functions, *Chem. Rev*., doi.org/10.1021/acs.chemrev.9b00550; (d) Y. Yuan, G. Zhu, *ACS Cent. Sci*., 2019, **3**, 409; (e) L. Tan and B. Tan, Hypercrosslinked porous polymer materials: design, synthesis, and applications, *Chem. Soc. Rev*., 2017, **46**, 3322.
5 (a) Q. Chen, M. Luo, P. Hammershoj, D. Zhou, Y. Han, B. Laursen, C. Yan and B. Han, Microporous polycarbazole with high specific surface area for gas Storage and separation, *J. Am. Chem. Soc*., 2012, **134**, 6084; (b) B. Li, Y. Zhang, R. Krishna, K. Yao, Y. Han, Z. Wu, D. Ma, Z. Shi, T. Pham, B. Space, J. Liu, P. K. Thallapally, J. Liu, M. Chrzanowski and S. Ma, Introduction of π-Complexation into porous aromatic framework for highly selective adsorption of ethylene over ethane, *J. Am. Chem. Soc*., 2014, **136**, 8654; (c) K. Huang, J. Zhang, F. Liu and S. Dai, Synthesis of porous polymeric catalysts for the conversion of carbon dioxide, *ACS Catal*., 2018, **8**, 9079; (d) M. M. Unterlass, F. Emmerling, M. Antoniettia and J. Webera, From dense monomer salt crystals to CO_2 selective microporous polyimides via solid-state polymerization, *Chem. Commun*., 2014, **50**, 430.
6 (a) S. J. Yang, X. Ding and B. H. Han, Conjugated microporous Polymers with extended π-Structures for organic vapor adsorption, *Macromolecules*, 2018, **513**, 947; (b) Z. Li, X. Feng, Y. Zou, Y. Zhang, H. Xia, X. Liu and Y. Mu, A 2D azine-linked covalent organic framework for gas storage applications, *Chem. Commun*., 2014, **50**, 13825; (c) N. Huang, P. Wang, M. A. Addicoat, T. Heine and D. Jiang, Ionic covalent organic frameworks: design of a charged interface aligned on 1D channel walls and its unusual electrostatic functions, *Angew. Chem. Int. Ed*., 2017, **56**, 4982.
7 (a) L. Chen, Y. Yang, D. Jiang, CMPs as scaffolds for constructing porous catalytic frameworks: a built-in heterogeneous catalyst with high activity and selectivity based on nanoporous metalloporphyrin polymers, *J. Am. Chem. Soc*., 2010, **26**, 9138; (b) K. Wu, J. Guo and C. Wang, An Elastic monolithic catalyst: a microporous metalloporphyrin-containing framework-wrapped melamine foam for process-intensified acyl transfer, *Angew. Chem. Int. Ed*., 2016, **55**, 6013; (c) Q. Sun, B. Aguila, G. Verma, X. Liu, Z. Dai, F. Deng, X. Meng, F. S. Xiao, and S. Ma, Superhydrophobicity: constructing, homogeneous catalysts into superhydrophobic porous frameworks to protect them from hydrolytic degradation, *Chem*, 2016, **1**, 628.
8 (a) X. Ding and B. Han, Metallophthalocyanine-based conjugated microporous polymers as highly efficient photosensitizers for singlet oxygen generation, *Angew. Chem. Int. Ed*., 2015, **54**, 6536; (b) R. S. Sprick, J.-X. Jiang, B. Bonillo, S. Ren, T. Ratvijitvech, P. Guiglion, M. A. Zwijnenburg, D. J. Adams and A. I. Cooper, Tunable organic photocatalysts for visible-light-driven hydrogen evolution, *J. Am. Chem. Soc*., 2015, **137**, 3265.
9 Z. Li, N. Huang, K. H. Lee, Y. Feng, S. Tao, Q. Jiang, Y. Nagao, S. Irle and D. Jiang, Light-emitting covalent organic frameworks: fluorescence improving via pinpoint surgery and selective switch-on sensing of anions, *J. Am. Chem. Soc*., 2018, **39**, 12374.
10 (a) S. Ding, M. Dong, Y. Wang, Y. Chen, H. Wang, C. Su and W. Wang, Thioether-based fluorescent covalent organic framework for selective detection and facile removal of mercury(II), *J. Am. Chem. Soc*., 2016, **138**, 3031; (b) J. Dong, X. Li, S. Bo Peh, Y. D. Yuan, Y. Wang, D. Ji, S. Peng, G. Liu, S. Ying, D. Yuan, J. Jiang, S. Ramakrishna and D. Zhao, Restriction of molecular rotors in ultrathin two-dimensional covalent organic framework nanosheets for sensing signal amplification, *Chem. Mater*., 2019, **31**, 146.
11 (a) Y. Ye, L. Zhang, Q. Peng, G. E. Wang, Y. Shen, Z. Li, L. Wang, X. Ma, Q. H. Chen, Z. Zhang and S. Xiang, High anhydrous proton conductivity of imidazole-loaded mesoporous polyimides over a wide Range from subzero to moderate temperature, *J. Am. Chem. Soc*., 2015, **2**, 913; (b) H. Xu, S. Tao and D. Jiang, Proton conduction in crystalline and porous covalent organic frameworks, *Nat. Mater*., 2016, **15**, 722; (c) H. Ma, B. Liu, B. Li, L. Zhang, Y. Li, H. Q. Tan, H. Y. Zang and G. Zhu, Cationic covalent organic frameworks: a simple platform of anionic exchange for porosity tuning and proton conduction, *J. Am. Chem. Soc*., 2016, **18**, 5897.
12 (a) S. Chandra, T. Kundu, S. Kandambeth, R. BabaRao, Y. Marathe, S. M. Kunjir and R. Banerjee, Phosphoric acid loaded azo (−N=N−) based covalent organic framework for Proton conduction, *J. Am. Chem. Soc*., 2014, **136**, 6570; (b) A. Halder, M. Ghosh, A. Khayum, S. Bera, M. Addicoat, H. S. Sasmal, S. Karak, S. Kurungot and R. Banerjee, Interlayer hydrogen-bonded covalent organic frameworks as high-performance supercapacitors, *J. Am. Chem. Soc*. 2018, **140**, 10941.
13 Y. Peng, G. Xu, Z. Hu, Y. Cheng, C. Chi, D. Yuan, H. Cheng and D. Zhao, Mechanoassisted synthesis of sulfonated covalent organic frameworks with high intrinsic proton conductivity, *ACS Appl. Mater. Interfaces*, 2016, **28**, 18505.
14 (a) D. W. Kang, K. S. Lim, K. J. Lee, J. H. Lee, W. R. Lee, J. H. Song, K. H. Yeom, J. Y. Kim and C. S. Hong, Cost-effective, high-performance porous-organic-polymer conductors functionalized with sulfonic acid groups by direct postsynthetic substitution, *Angew. Chem. Int. Ed*., 2016, **55**, 16123; (b) C. Klumpen, S. Gödrich, G. Papastavrou and J. Senker, Water mediated proton conduction in a sulfonated microporous organic polymer, *Chem. Commun*., 2017, **53**, 7592; (c) P. Samanta, A. V. Desai, B. Anothumakkool, M. M. Shirolkar, A. Karmakar, S. Kurungot and S. K. Ghosh, Enhanced proton conduction by post-synthetic covalent modification in a porous covalent framework, *J. Mater. Chem. A*, 2017, **5**, 13659.
15 (a) S. J. Yang, X. Ding and B. H. Han, Conjugated microporous polymers with dense sulfonic acid groups as efficient proton conductors, *Langmuir*, 2018, **26**, 7640; (b) D. W. Kang, K. A. Lee, M. Kang, J. Min Kim, M. Moon, J. H. Choe, H. Kim, D. W. Kim, J. Y. Kim and C. S. Hong, Cost-effective porous-organic-polymer-based electrolyte membranes with superprotonic conductivity and low activation energy, *J. Mater. Chem. A*, 2020, **8**, 1147.
16 (a) B. Li, R. Gong, W. Wang, X. Huang, W. Zhang, H. Li, C. Hu and B. Tan, A new strategy to microporous polymers: knitting rigid aromatic building blocks by external cross-linker, *Macromolecules*, 2011, **44**, 2410; (b) S. Yao, X. Yang, M. Yu, Y. Zhang and J. X. Jiang, High surface area hypercrosslinked microporous organic polymer networks based on tetraphenylethylene for CO_2 capture, *J. Mater. Chem. A*, 2014, **2**, 8054; (c) X. Jing, D. Zou, P. Cui, H. Ren and G. Zhu, Facile synthesis of cost-effective porous aromatic materials with enhanced carbon dioxide uptake, *J. Mater. Chem. A*, 2013, **1**, 13926.
17 T. A. Zawodzinski, Jr, C. Derouin, S. Radzinski, R. J. Sherman, V. T. Smith, T. E. Springer and S. Gottesfeld, Water uptake by and transport through Nation 117 membranes, *J. Electrochem. Soc*., 1993, **140**, 1041.

18 (a) J. Peron, A. Mani, X. Zhao, D. Edwards, M. Adachi, T. Soboleva, Z. Shi, Z. Xie, T. Navessin, S. Holdcroft, Properties of Nafion NR-211 membranes for PEMFCs, *J. Membr. Sci.* 2010, **356**, 44; (b) K. M. Nouel, P. S. Fedkiw, Nafion®-based composite polymer electrolyte membranes, *Electrochim. Acta*, 1998, **43**, 2381.